PHILOSOPHICAL TRANSACTIONS OF THE ROYAL SOCIETY A MATHEMATICAL, PHYSICAL & ENGINEERING SCIENCES

Wind-Induced Instability of Structures [and Discussion]

G. V. Parkinson and D. Dicker

Phil. Trans. R. Soc. Lond. A 1971 **269**, 395-413
doi: 10.1098/rsta.1971.0040

Phil. Trans. Roy. Soc. Lond. A. **269**, 395–409 (1971) [395]
Printed in Great Britain

Wind-induced instability of structures

By G. V. Parkinson
Department of Mechanical Engineering, The University of British Columbia, Vancouver, Canada

[Plate 10]

Forms of wind-induced instability of structures are described, and two of these, typical of long bodies with bluff cross-sections, are selected for more detailed consideration. The first is vortex-induced bending oscillation, a type of resonant response to the periodic surface pressure loading caused by the discrete wake vortex street formed from the shear layers separating from the bluff cross-section. Oscillation phenomena are described, including capture of the vortex frequency by the structural response frequency over a discrete wind speed range and amplification and phase shift of the loading over this range. The second form is transverse galloping, arising from aerodynamic instability of the bluff cross-sectional shape, so that small-amplitude oscillations generate forces which increase the amplitudes to large values. Oscillation phenomena are described, including the occurrence at very nearly natural frequencies, and the relatively large amplitudes (compared to vortex-induced oscillations) increasing with wind speed beyond a critical wind speed dependent on the level of structural damping. Effects of body and wind parameters on both forms of oscillation are considered, and methods of analysis and suppression for susceptible structures are described. Some probable future requirements and prospects are considered.

1. Introduction

It has been regrettably common in engineering practice for structures, demonstrably strong enough to resist the steady loads expected from wind action, to display instead some form of instability leading to discomfort, damage, or destruction under the action of real winds. These instabilities are to be distinguished from the response of structures to the random buffeting by fluctuating pressure loads arising from the turbulence in natural winds. Each form of instability represents a coherent interaction between the structure and the wind.

Most forms are oscillatory, but divergent instabilities are possible. One such form is the buckling collapse under wind pressure of cylindrical shell structures. There have been fairly recent incidents in England of cylindrical steel tanks collapsing in this way while under erection, and the phenomenon has been studied by Holownia (1968).

For oscillatory instabilities of structures, the commonest source of excitation is the organized wake vortex system. Most structures are aerodynamically bluff, so that in wind the flow separates from their surface to form a wake with breadth of the order of that of the structure. The separating shear layers are unstable and roll up to form discrete vortices. If the structure is relatively long, and the wind is approximately normal to the long dimension, these vortices, as they are swept downstream by the flow, form two parallel rows with equal vortex spacing, those in one row opposite the mid-points of the spaces in the opposite row. For a particular structure, the vortices in each row form at a frequency f_v proportional to the incident wind speed V and inversely proportional to the lateral dimension h, so that a characteristic number, the Strouhal number

$$S = f_v h/V$$

is associated with each structural shape.

As a consequence of this discrete wake vortex formation, the flow field has a dominant periodicity, and the structure generating the wake is exposed to a periodic pressure loading which results in a transverse, or lift force at frequency f_v, arising from the asymmetry of the vortex

formation, and a weaker drag force at frequency $2f_v$. Accordingly, if the structure is elastic with natural frequencies f_n near f_v or $2f_v$, it will tend to develop a resonant response in the form of bending oscillations normal to or parallel to the wind direction. Moreover, if the structural cross-section is relatively flexible, it may develop resonant breathing oscillations. These are described as ovalling oscillations when they occur at the open ends of circular cylindrical shells such as smoke stacks, and they have been investigated by Johns & Allwood (1968), among others.

A second important class of wind-induced oscillatory instabilities is, rather appropriately, called galloping, because of the visual impression given by its typical low-frequency, high-amplitude occurrence. Galloping arises from an instability of the aeroelastic system to small displacements of the elastic structure. It also occurs for long structures with aerodynamically bluff cross-sections, and it requires only one degree of freedom, either bending with translation of the structural section normal to its span and to the wind direction, or torsion about a spanwise axis. In galloping, when an unstable elastically restrained section is given a small translational or angular velocity in the presence of a steady wind normal to the span, an increment of transverse force or torque develops which acts in the direction of the motion, so that an oscillation builds up, the final amplitude depending on the force or torque variation with attitude of the sectional shape, and on the structural damping.

The final catastrophic oscillation of the original Tacoma Narrows Suspension Bridge in 1940 was an example of torsional galloping. The commonly observed large-amplitude vertical oscillations of ice-laden transmission lines in winter represent translational galloping. A third form of galloping, essentially translational, can occur for stranded conductors in a wind directed a few degrees from the normal to the span. The lift force exciting this form arises from the differing angular positions of flow separation from the conductor on opposite sides, because of the differing surfaces presented to the flow by the helically wound strands. It occurred spectacularly 10 years ago on transmission lines crossing the Rivers Severn and Wye, and was subsequently investigated thoroughly (Davis, Richards & Scriven 1963). A fourth form of galloping in one degree of freedom may be identified. It is referred to as stall flutter because of its occurrence for airfoils oscillating about their stalling angle. Its excitation involves a hysteresis in the separation and reattachment of the air flow as the body oscillates about the stalling angle, and it has been observed in model experiments on bowl-shaped structures such as are used for radio telescopes (Scruton 1968).

The class of wind-induced oscillatory instabilities usually referred to as flutter is more complex in that motions in two or more degrees of freedom are necessarily involved. Individual degrees of freedom have stable motions, but the aerodynamic, elastic, and/or inertial couplings between the degrees of freedom permit the extraction of energy from the wind to produce the combined unstable motions. Flutter of airplane wings involving bending and twisting motions has been a recurring problem through the history of aviation, and this form, now usually called classical flutter, can occur for other wing-like structures, such as the welded-box deck structures increasingly used in suspension bridge design (Walshe 1964). A related form of flutter has been observed on transmission lines employing the horizontal twin-conductor arrangement. This has been investigated by Simpson & Lawson (1968).

Of the above forms of wind-induced instability, some are fairly easily eliminated in design if adequate information on local winds is available (buckling collapse, ovalling), or easily cured (yaw-dependent galloping of stranded conductors, by wrapping them smoothly with tape). Some are less significant (vortex-induced oscillation in the wind direction) or are very similar to another form (stall flutter and torsional galloping to transverse galloping). Flutter is important, but

PHILOSOPHICAL TRANSACTIONS OF THE ROYAL SOCIETY A MATHEMATICAL, PHYSICAL & ENGINEERING SCIENCES

relatively rare in architectural aerodynamics, and its complexity makes a detailed discussion inappropriate to the scope of the present paper. The remaining forms, vortex-induced bending oscillations and transverse galloping, will be considered in some detail in the following sections.

2. Vortex-induced transverse bending oscillations

(a) *Phenomena of the oscillations*

Some phenomena of the vortex-induced transverse bending oscillations of bluff cylindrical bodies depend in detail on the cross-sectional shape of the body and on structural and wind

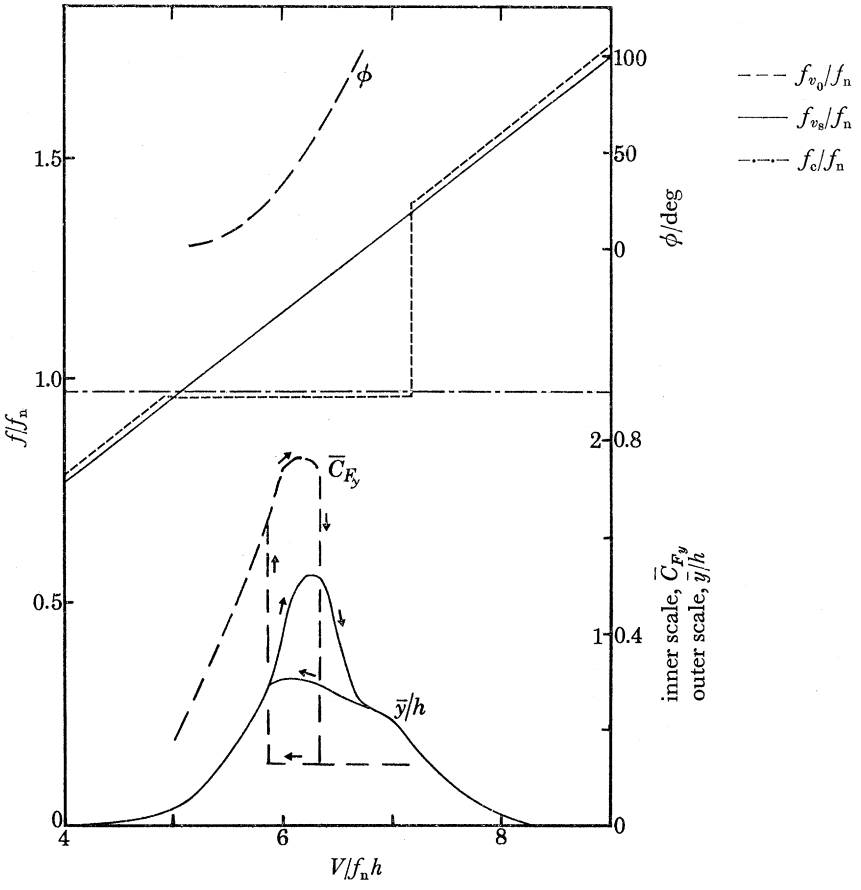

Figure 1. Phenomena of vortex-induced oscillation.

parameters. However, certain features of the oscillations are common to all cross-sections and conditions, and are conveniently discussed for the circular cylinder, the most intensively studied structural shape.

Figure 1, based on recent measurements (Ferguson & Parkinson 1967; Feng 1968) on circular cylinders at subcritical Reynolds numbers under approximately two-dimensional conditions, summarizes several of these common features. The first significant feature is the occurrence of oscillations only in discrete ranges of wind speed V, each range containing a wind speed V^* for which the wake vortex frequency f_{v_s} for the stationary cylinder coincides with a natural frequency f_n of the elastic system. One such range is shown in figure 1, and f_{v_s} is seen to equal f_n at slightly above the lowest wind speed for which oscillation begins. Maximum oscillation amplitude $\bar{y}$ is

seen to occur for a wind speed about 30 % higher than V^*, and oscillation ceases for wind speeds more than 70 % higher than V^*. The cylinder oscillates at a frequency f_c very close to f_n throughout the range.

The vortex frequency during cylinder oscillation, however, does not have its stationary-cylinder value f_{vs}, corresponding to $S = 0.198$, through the oscillation range. At wind speeds initiating very low cylinder amplitudes, f_{v_0} equals f_{vs} and is slightly less than f_c, leading to the beat modulation of cylinder amplitude and fluctuating surface pressure amplitude shown in figure 2, plate 10, extracted from Feng (1968). If the wind speed is increased slightly, with a corresponding small increase in amplitude $\bar{y}$, f_{v_0} is captured by f_c, and this capture persists over most of the wind-speed range giving oscillation, including V for maximum $\bar{y}$. However, at slightly higher wind speed, with the cylinder still oscillating with large amplitude, f_{v_0} suddenly reverts to f_{vs} and follows the stationary-cylinder variation over the remainder of the oscillation range.

The excitation for these oscillations is the organized surface pressure distribution on the cylinder, fluctuating asymmetrically with fundamental frequency f_{v_0} and giving a periodic transverse force F_y per unit cylinder span conveniently described by a coefficient C_{F_y} defined by

$$F_y = C_{F_y} \tfrac{1}{2} \rho V^2 h, \tag{1}$$

where ρ is fluid density. In the capture range, C_{F_y} oscillates with cylinder frequency f_c, and a phase angle ϕ by which C_{F_y} leads displacement y can be defined, so that, if

$$y = \bar{y} \sin 2\pi f_c t, \tag{2}$$

then

$$C_{F_y} = \bar{C}_{F_y} \sin (2\pi f_c t + \phi), \tag{3}$$

and the behaviour of the excitation during capture can be presented in terms of ϕ and amplitude $\bar{C}_{F_y}$. Figure 1 shows the large increase in $\bar{C}_{F_y}$ with $\bar{y}$ towards maxima, with the subsequent abrupt drop of $\bar{C}_{F_y}$ to values typical of the excitation on stationary cylinders, and the nearly linear increase of ϕ from 0 to over 100°. Recent measurements by Hartlen, Baines & Currie (1968) are in general agreement with the phenomena of figure 1. Results of Bishop & Hassan (1964), although not directly comparable in all respects because of the different experiments performed, show agreement with the above variation of ϕ. Figure 3, plate 10, taken from Feng (1968), shows the abrupt change in excitation near maximum cylinder amplitude. In figures 3*a*, *b* and *c*, the dimensionless wind speed $V/f_n h$ is increased from 6.33, the value for $\bar{y}_{max}$, to 6.68 and, as $\bar{y}$ gradually decreases from $\bar{y}_{max}$, the amplitude of surface pressure fluctuation at a tap located on the transverse diameter abruptly decreases from a high value with some random modulation to a much lower constant value. When the wind speed is reduced, some oscillation hysteresis is evident, and, although $\bar{y}$ increases, it does not reach as high values as when wind speed was increasing, as shown in figure 1. The surface pressure amplitude jumps abruptly to a higher value, but not until $V/f_n h$ is reduced from 6.11 to 5.89, as shown in figure 3*d*.

It is well known that the fluctuating surface pressure on a stationary cylinder has large random amplitude modulation, and simultaneous pressure signals at two points on a spanwise line are poorly correlated. In the high-amplitude range of cylinder oscillation, with vortex frequency captured, not only is the amplitude modulation greatly reduced, as shown in figure 3, but the spanwise correlation is greatly increased, making flow conditions more nearly two-dimensional. Figure 4 shows a comparison taken from Feng (1968) of conventionally defined normalized two-point correlation (unity is perfect correlation) as a function of spanwise separation for a circular cylinder at rest and in maximum amplitude vortex-induced oscillation. These results are in good agreement with other measurements (Toebes 1969).

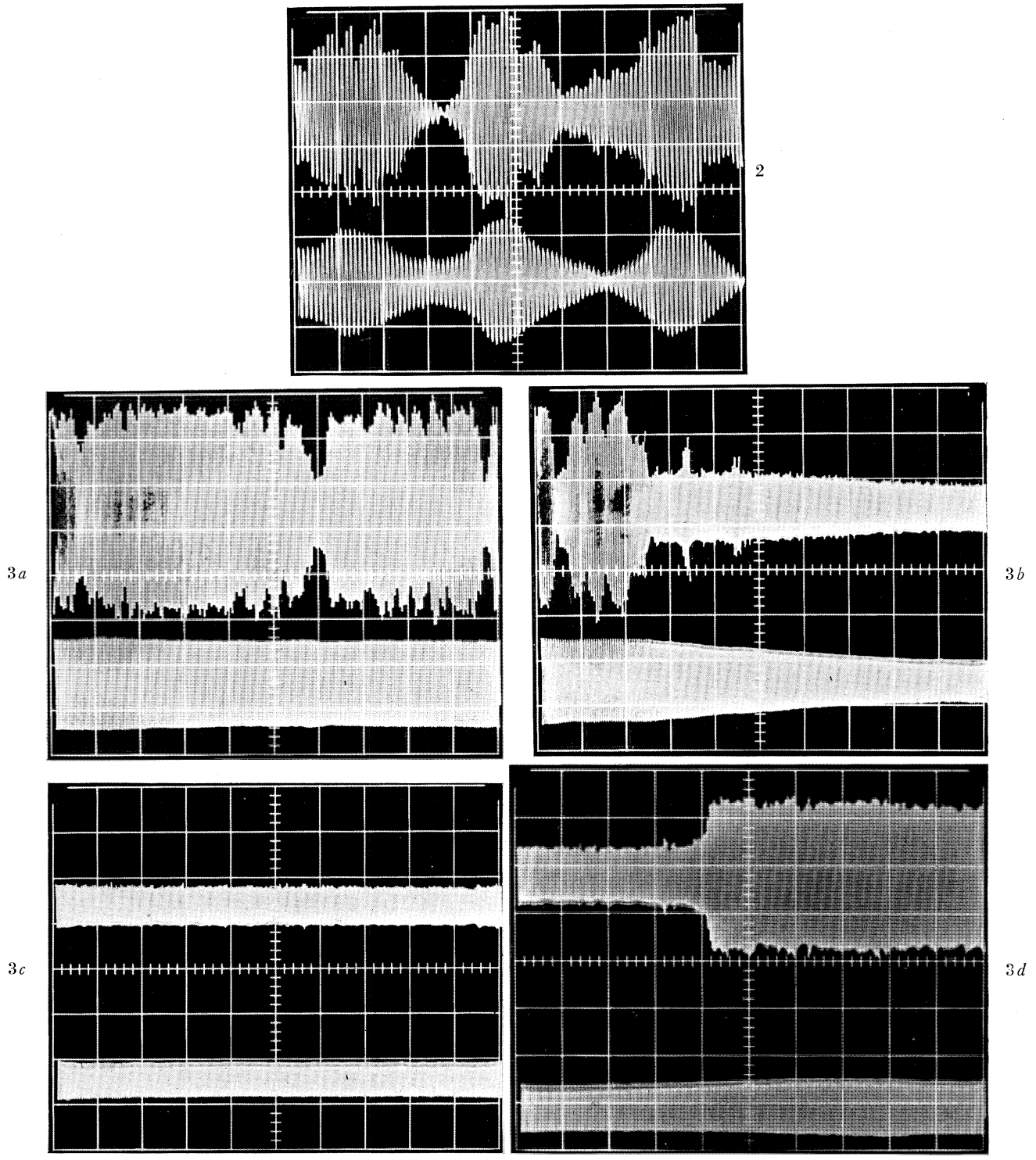

FIGURE 2. Beat phenomenon. $V/f_n h = 4.97$. Upper trace: surface pressure at transverse tap, $f_{v_0} = 8.73$ Hz. Lower trace: cylinder displacement, $f_c = 9.04$ Hz. Time base: 1 s/division.

FIGURE 3. Transient effects on cylinder and surface pressure amplitudes during capture. Upper traces: surface pressure at transverse tap, $f_{v_0} = 9.04$ Hz. Lower traces: cylinder displacement, $f_c = 9.04$ Hz. Time base: 2 s/division. (*a*) $V/f_n h = 6.33$; (*b*) $6.33 < V/f_n h < 6.68$. (*c*) $V/f_n h = 6.68$. (*d*) $6.11 > V/f_n h > 5.89$.

(*Facing p.* 398)

Further evidence of the spanwise correlating effect of cylinder oscillation is obtained from the geometry of the wake vortices. The vortices from stationary cylinders, viewed normal to the plane of the cylinder axis and flow direction, have been observed to exhibit slantwise formation, with the vortex filaments at small angles to the cylinder axis (Gerrard 1966; Koopmann 1967). Feng (1968) has found that this slantwise formation persisted at small cylinder oscillation amplitudes, but changed to formation parallel to the cylinder axis at larger amplitudes. This change is confirmed by Koopmann (1967).

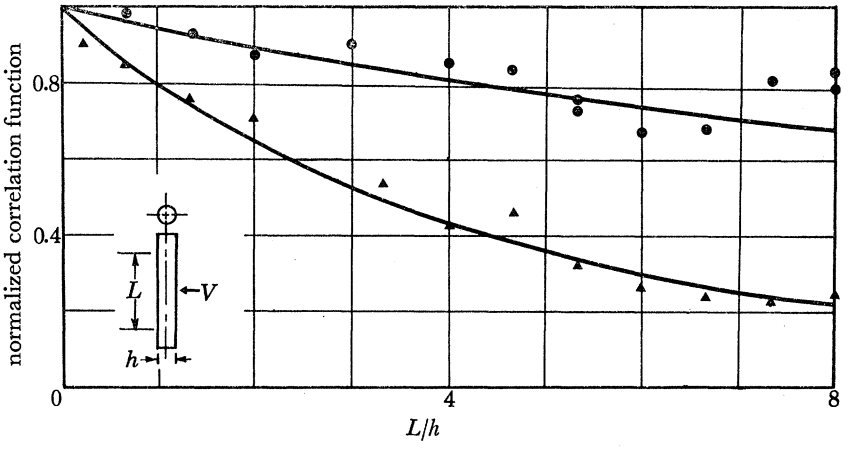

FIGURE 4. Normalized two-point spanwise correlations for stationary and oscillating circular cylinder. $V/f_n h = 6.11$. $Re = 21\,000$. ▲, stationary cylinder; ●, oscillating cylinder, $\bar{y}/h = 0.4$.

(*b*) *Effects of body and incident wind parameters*

Structural and wind parameters cause quantitative differences in the phenomena of § 2*a*. A long elastic structure will usually have several natural frequencies that could be excited by wake vortices, each one corresponding to a capture range of wind speeds over which oscillation in the corresponding mode could occur. The original Tacoma Narrows Suspension Bridge exhibited many modes of vortex-excited bending oscillation in the months previous to its final catastrophic torsional oscillation (Farquharson, Smith & Vincent 1949–54).

The structural damping is an important parameter, since a sufficiently high value completely eliminates vortex-induced oscillations. Its effect is conveniently shown on the form of stability diagram used by Scruton (1965), and figure 5, taken from Feng (1968), shows two such diagrams for the circular cylinder and the semi-circular, or D-section, cylinder. The abscissa,

$$\Delta = 2\pi\beta/n,$$

is a dimensionless structural damping parameter in which β is the damping as a fraction of critical damping (the level of damping which would eliminate free oscillations of the structure) and n is a number proportional to the ratio of fluid to structural density. The solid curves mark stability boundaries within which $\bar{y}$ is greater than 1 % of diameter h. The dotted curve indicates $\bar{y}_{max}$.

The structural shape is obviously important. The nature of the span of a long elastic body is significant—whether it is cantilevered, as in a mast, tower, or smokestack, or supported at both ends, as in a suspension bridge deck or a structural member. Model studies of these phenomena are commonly made on rigid sectional models in wind tunnels, with artificial external elastic and damping parameters. This approach assumes locally two-dimensional flow on the prototype structure, apparently a reasonable assumption for the structures supported at both ends. One might, however, expect some aerodynamic effects of the length: diameter ratio and of the tip

shape for cantilevered towers or stacks. For circular cylinders, Hartlen *et al.* (1968) found such effects to be small for smooth cylinders longer than 10 diameters, tested at subcritical Reynolds number, although they found a different type of oscillation hysteresis than that described in §2*a*, whereas Wootton (1968) found appreciable effects on rough and smooth cylinders ranging in length from 8 to 11.5 diameters, tested at high subcritical and supercritical Reynolds numbers.

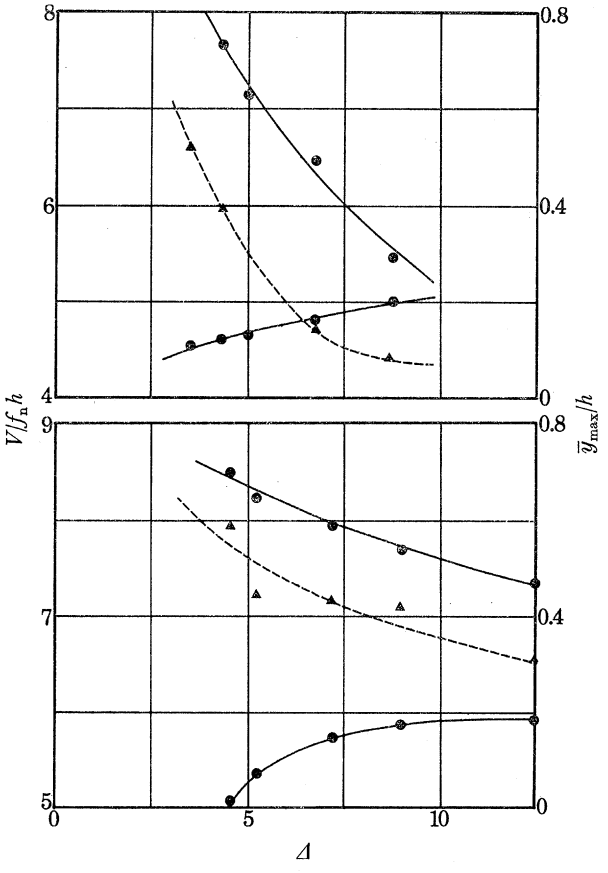

FIGURE 5. Stability boundaries for circular and D-section cylinders. (*a*), circular cylinder; (*b*) D-section cylinder ; —●—, stability boundary for $\bar{y}/h = 0.01$; – –▲– –, $\bar{y}_{max}/h$.

For a tapered cylindrical tower or stack, the capture range of large-amplitude oscillation appears to be determined by the Strouhal number based on the tip diameter (Scruton 1965).

More important than the nature of the span is the cross-sectional shape. All cross-sections have characteristic Strouhal numbers, which in general vary with the attitude of the section to the wind and with the Reynolds number. If the section has sharp corners, the flow separation will usually occur there, with two effects on the wake vortex system. First, there will be little Reynolds number influence on the near-wake geometry, so the Strouhal number will be nearly independent of Reynolds number. Secondly, the vortex formation will be well correlated along the span, so the excitation will be stronger and more coherent than for a rounded section, whose flow separation is determined by boundary-layer Reynolds number effects. This can be seen in figure 5, where the sharp corners of the D-section have produced stronger vortex excitation and a considerably more unstable oscillator than the circular section.

Another important sectional shape parameter is the streamwise length and the shape of the part of the section downstream of the separation points, since this afterbody is the part of the

structure most directly exposed to the vortex excitation. Thus, the D-section with flat face upstream experiences large excitation, as in figure 5, but with flat face downstream the excitation is negligible, and no oscillation occurs. This effect has also been observed by Slater (1969) on a symmetrical structural angle section, for which large vortex-induced oscillations occurred with the angle vertex downstream, but oscillations were barely perceptible with the vertex upstream. A long afterbody will either interfere with the wake vortex formation or cause the separated flow to reattach to its surface, and separate again downstream, with vortex formation

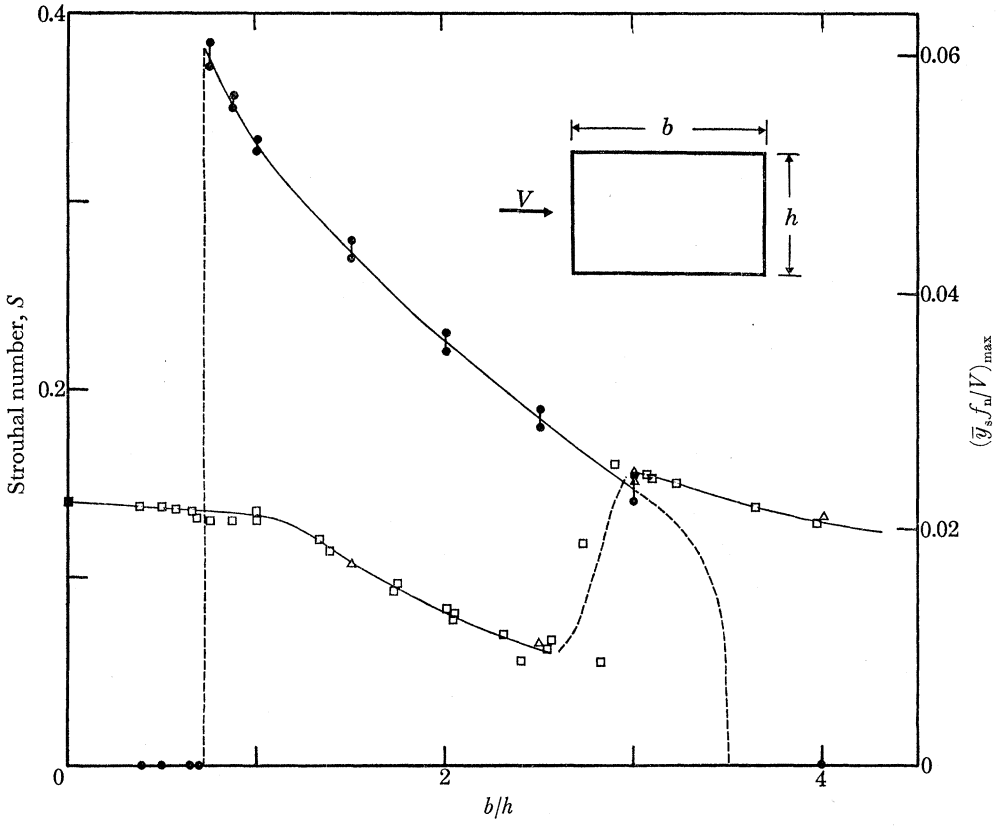

FIGURE 6. Effects of rectangular section afterbody length. Strouhal number S: ■, Roshko (1954); □, Brooks (1960); △, Smith (1962). Maximum ratio of cylinder amplitude to wind speed $(\bar{y}_s f_n/V)_{max}$: ❙, Brooks (1960), Smith (1962).

delayed to the wake of the second separation. In either case the Strouhal number is directly affected by this parameter, as shown in figure 6, based on measurements by Roshko (1954), Brooks (1960), and Smith (1962) for a family of rectangles.

Reynolds number $Re = Vh/\nu$ for flow past a cylinder, where ν is fluid kinematic viscosity, is an important parameter for rounded sections, where both the Strouhal number and the afterbody size are determined by the movement of the separation points with Re. Measurements on stationary circular cylinders indicate mean separation points at about 82° from the front, and a constant value of S of about 0.20, over the approximate Reynolds number range $10^3 < Re < 10^5$, the subcritical range. Most model experiments, including those from which results are presented here, are performed in this range. In the critical and supercritical ranges, approximately $10^5 < Re < 3 \times 10^6$, there are laminar separation bubbles with final turbulent separation delayed to about 120° from the front, so that the wake is narrow and the afterbody small. Finally, in

what Roshko (1961) has called the transcritical range $Re > 3 \times 10^6$, the bubbles are eliminated and turbulent separation occurs at about 100° from the front. These different ranges produce considerably different Strouhal numbers and excitations on stationary cylinders. Wootton (1968) found, however, in tests on roughened cylindrical stacks, that if structural damping was low enough to permit large-amplitude oscillations, the subcritical Strouhal number of 0.20 appeared to govern the oscillation phenomena at all Reynolds numbers.

He also found large-amplitude oscillations of smooth cylindrical stacks at supercritical Reynolds numbers for which $V/f_n h$ was between 10 and 13, in addition to the usual range around 5, and he concluded that there were important quantitative effects of Reynolds number on vortex-induced oscillations.

Turbulence in the incident wind is another important parameter in vortex-induced oscillations, but its effects on the vortex excitation and response should probably be considered in the context of the general response of the structure to the turbulence, and are therefore outside the scope of the present paper. Davenport (1961) has been a major contributor to this general problem in recent years.

(*c*) *Methods of analysis and suppression*

The analysis of separated flows about bodies remains semi-empirical, particularly for time-dependent flows about oscillating bodies, because of the unavailability of analytical models to represent the characteristics of the wake as determined by the body and its motions. Therefore, whereas a satisfactory body of theory, for both the aerodynamics and the body motions, is available to predict flutter characteristics for streamlined airfoils (Fung 1955), the available aerodynamic information for wind-induced oscillations of bluff bodies is mainly empirical, so that wind tunnel tests of scale models are the engineer's main tool, and the analyses of the oscillations accordingly involve empirically determined excitations of the dynamical systems.

For vortex-induced oscillations of structures it is usually reasonable to consider the structure as a linear dynamical system, so that elastic restoring force is proportional to oscillatory displacement y, and structural damping force is proportional to oscillatory velocity $\mathrm{d}y/\mathrm{d}t$. The excitation is periodic, and approximately simple harmonic, so that, if C_{F_y} in equation (1) had constant amplitude $\bar{C}_{F_y}$ and frequency f_{v_0}, a simple linear equation for y would result, with $\bar{C}_{F_y}$ and f_{v_0} supplied empirically, from experiments on stationary cylinders. However, $\bar{C}_{F_y}$ and f_{v_0} were seen in § 2*a* to depend on cylinder amplitude $\bar{y}$, so the governing dynamical system is nonlinear, and, with the additional empiricism required by this motion dependence of the aerodynamic parameters, much more difficult. Hartlen *et al.* (1968) have made a significant contribution to this analysis by assuming y and C_{F_y} to be coupled weakly nonlinear oscillators of simple form in the capture range. They tested the resulting semi-empirical theoretical model by calculating, $\bar{y}, f_e, \phi$, and $\bar{C}_{F_y}$ as functions of $V/f_n h$ for the parameters of the present figure 1, and found good agreement with most features of the observed variations.

Architects and most engineers studying vortex-induced oscillations are interested in diagnosis only in so far as it contributes to prevention or cure, and even rather primitive analysis can indicate possible approaches. Thus, if equations (2) and (3) for the capture range are substituted in the equation of motion for the linear dynamical system postulated above, it follows, using the fact that f_e is nearly equal to the system natural frequency f_n, that

$$\frac{\bar{y}}{h} \doteq \frac{1}{4\pi} \frac{\bar{C}_{F_y}}{\Delta} \left(\frac{V}{f_n h} \right)^2 \sin \phi. \tag{4}$$

PHILOSOPHICAL TRANSACTIONS OF THE ROYAL SOCIETY A MATHEMATICAL, PHYSICAL & ENGINEERING SCIENCES

Near $\bar{y}_{max}$, $\sin\phi$ will be close to unity, so large amplitudes must be avoided by reducing $\bar{C}_{F_y}$, increasing Δ, or avoiding the critical range (or ranges) of $(V/f_n h)$.

Since $(V^*/f_n h) = 1/S$, and V for $\bar{y}_{max}$ is close to V^*, it is sometimes possible to raise V^* out of the range of probable wind speeds by sufficiently increasing the lowest natural frequency f_n of the structure. An alternative structural approach is to increase Δ by increasing β or decreasing n, or both. Either of these approaches can completely eliminate vortex-induced oscillations if the required increases in f_n or Δ are compatible with other structural or aesthetic features of the installation.

The third approach, to reduce $\bar{C}_{F_y}$, requires aerodynamic modifications to the design, and the usual method is to add some form of spoiler to inhibit the vortex formation and decrease the spanwise correlation of the fluctuating surface pressures. One type of spoiler easily applicable to circular cylinders is some form of helical spiral barrier wound around the cylinder. A form recommended by some (Nakagawa, Fujino, Arita & Shima 1965) consists of relatively small diameter wires or cables. This has proved unreliable, and a form of helical spoiler proposed by Scruton & Walshe (1957) has been much more successful. It consists of a series of sharp-edged rectangular-section fences, or strakes, wound around the cylinder and, in its best form (Scruton 1965), it eliminates vortex-induced oscillations at all wind speeds. This system has been applied successfully to a number of smokestacks, where typically only the top third of the stack is modified.

3. Transverse galloping oscillations

(a) *Phenomena of the oscillations*

Galloping oscillation in wind, like vortex-induced, occurs at a frequency very close to a structural natural frequency f_n, and has a nearly simple harmonic waveform. It also occurs with long elastic structures of aerodynamically bluff cross-section. An observer of an oscillating cylinder susceptible to both vortex-induced and galloping oscillations would be unable to determine which form was present unless the amplitude $\bar{y}$ was appreciably greater than the transverse cylinder dimension h. For while vortex-induced oscillations are typically limited to amplitudes $\bar{y}$ less than h, galloping amplitudes can be many times h, more than 100 times in observed instances of galloping of ice-covered transmission lines. Moreover, while vortex-induced oscillations occur only in discrete ranges of wind speed, galloping will occur at all wind speeds above a critical value determined by the structural damping.

Transverse galloping of a long elastic structure results from an aerodynamic instability of the bluff cross-section to its own transverse disturbance velocity $\mathrm{d}y/\mathrm{d}t$ in the presence of wind normal to the span. It will occur readily for a sectional shape that has fixed separation points and a reasonably long afterbody (in the sense of § 2 *b*). For such a shape, any lateral movement of the section will create a surface pressure distribution that gives a force F_y in the direction of $\mathrm{d}y/\mathrm{d}t$, so that displacement y is increased against the elastic restraint, and an oscillatory motion at a frequency close to f_n develops and increases in amplitude $\bar{y}$ until the energy dissipated per cycle by structural damping balances the energy input per cycle from the wind. Since this energy input increases with wind speed V, so does the stable galloping amplitude $\bar{y}_s$.

Just as the circular section is suitable for studying vortex-induced oscillations, so is the square section for studying galloping. Figure 7 shows a square section at rest and in transverse motion in the presence of a wind normal to a face and the plane of the motion. In figure 7*a* the section is at rest. The flow separates symmetrically from corners 1 and 4, and F_y is zero because of the

PHILOSOPHICAL TRANSACTIONS OF THE ROYAL SOCIETY A MATHEMATICAL, PHYSICAL & ENGINEERING SCIENCES

symmetrical pressure distribution. (That is, the time-averaged flow and pressure distribution are symmetrical, although the usual vortex-induced transverse fluctuations are present. Galloping typically occurs at wind speeds for which f_{vs} is much higher than f_n, where the effect of the vortex excitation has been shown to be negligible (Santosham 1966)). In figure 7*b* the section is moving

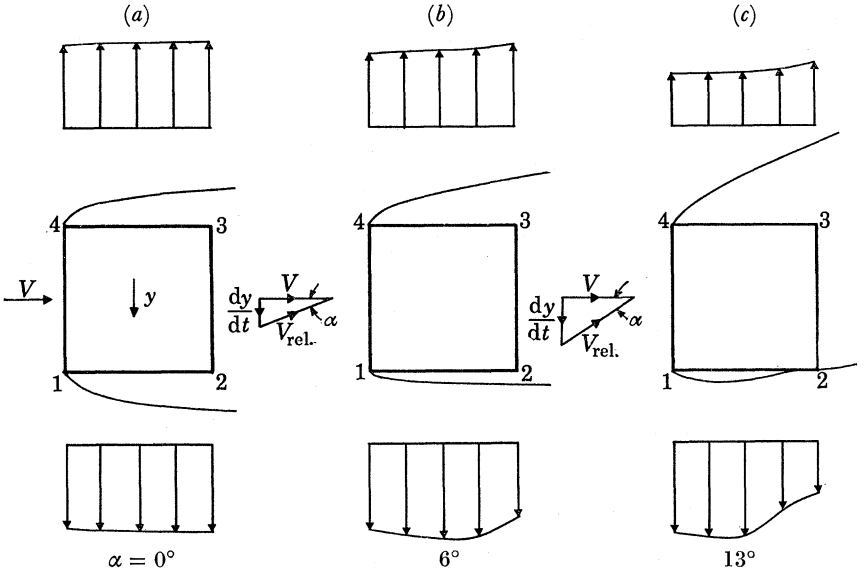

FIGURE 7. Effects of square section afterbody on separated shear layers during galloping. Pressure distributions on sides are shown to scale.

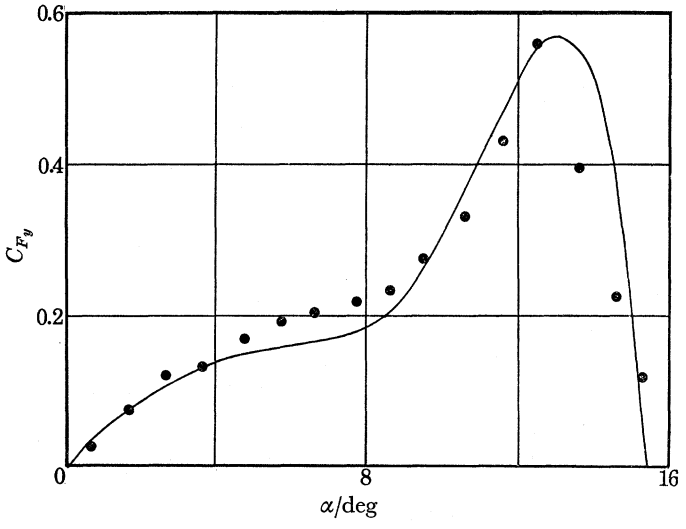

FIGURE 8. Transverse force coefficient C_{F_y} as a function of angle of attack α for square section. ●, experimental points (Smith 1962), $Re = 22\,300$; ——, polynomial approximation (Parkinson & Smith 1964).

down with velocity dy/dt such that the relative wind velocity V_{rel} is at an angle of attack α of 6°. The flow still separates at corners 1 and 4, but now the separated shear layers are asymmetric, the windward one lying closer to side 12 than the leeward one does to side 34. As a result, side 12 experiences a higher suction from the vorticity trapped adjacent to it than does 34, and there is a considerable force F_y in the direction of dy/dt. In Figure 7*c* the relative α is increased to 13°, and the flow has reattached on the windward side at 2. F_y reaches its maximum value at this angle,

as higher α causes the reattachment point on side 12 to move forward, reducing the net suction on that side.

Figure 8 shows the variation of coefficient C_{F_y} (defined as in equation (1)) with α for the square section. The experimental points were obtained from a wind tunnel test on a stationary cylinder (Parkinson & Smith 1964), since a fundamental assumption in the study of galloping is that the quasi-steady approximation is accurate—i.e. that the aerodynamics of figure 7 are nearly

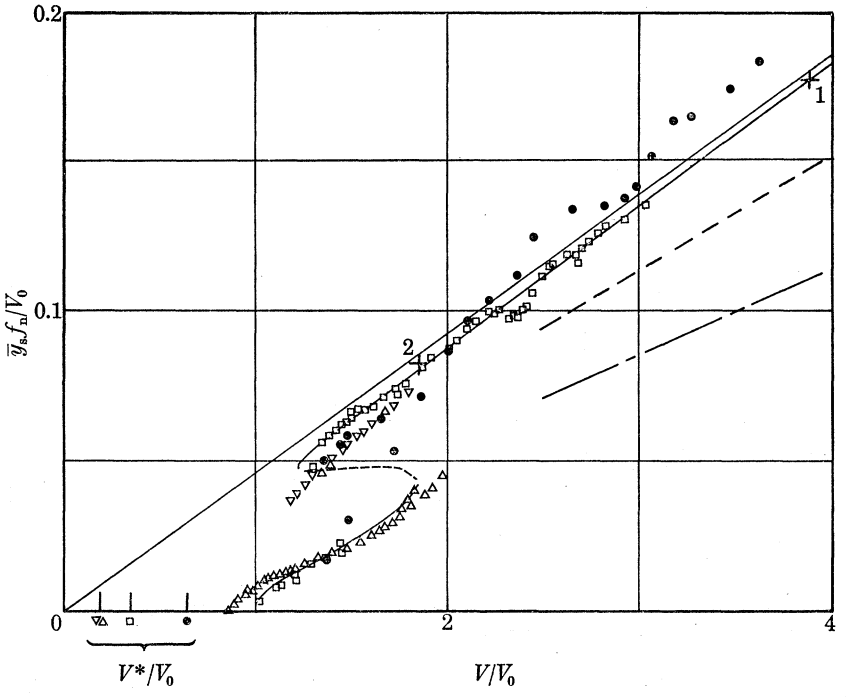

FIGURE 9. Reduced galloping amplitude $\bar{y}_s f_n/V_0$ as a function of reduced wind speed V/V_0 for square section. Experiments (Smith 1962): ●, $\beta = 0.00107$; □, $\beta = 0.00196$; △, $\beta = 0.00364$; ▽, $\beta = 0.00372$; +1, $\beta = 0.0012$; +2, $\beta = 0.0032$. $4000 < Re < 20000$. $n = 0.00043$. Theory (Parkinson & Smith 1964): ——, stable limit cycle; – – – –, unstable limit cycle. Experiments (Novak 1968): – – – –, 4.7% turbulence; — — — — —, 8.6% turbulence.

identical with the aerodynamics of the stationary cylinder at the appropriate α. The instability of the square section in the attitude $\alpha = 0°$ is shown by the positive slope of the curve

$$\left.\frac{\mathrm{d}C_{F_y}}{\mathrm{d}\alpha}\right|_{\alpha=0} = A > 0. \tag{5}$$

This instability criterion was first applied to galloping by den Hartog (1930), although Glauert (1919) had previously applied it to the analogous aerodynamic problem of auto-rotation of a stalled airfoil.

Figure 9 shows the results of wind tunnel tests of galloping for cylinders of square section (Parkinson & Smith 1964) in which stable amplitudes $\bar{y}_s$ are plotted against wind speed V for several levels of structural damping. The data are plotted in a dimensionless form arising from the theory of § 3*c*, in which

$$V_0 = (2\Delta/A) f_n h \tag{6}$$

is the theoretical critical wind speed initiating galloping. It can be seen that the galloping occurs at higher wind speeds than vortex-induced oscillations of the square cylinder, which occur near V^*.

There is some oscillation hysteresis in the galloping behaviour at low wind speeds, but at higher speeds $\bar{y}_s$ becomes proportional to V, a typical phenomenon of galloping.

Figure 10 shows the observed amplitude–time variation for the buildup of galloping from rest at two wind speeds, the tests identified as 1 and 2 in figure 9. The large number of cycles required to reach $\bar{y}_s$ in each case is also typical of galloping.

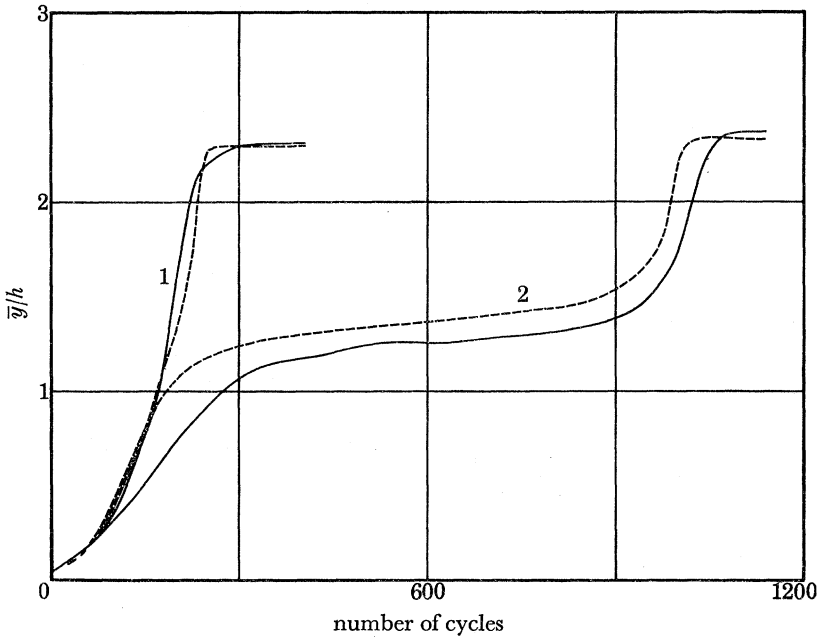

FIGURE 10. Buildup of galloping amplitude with time. ——, experiments (Smith 1962); – – – –, theory (Parkinson & Smith 1964).

This transverse form of galloping occurs commonly with ice-covered transmission lines, where the shape of the ice film provides the required unstable C_{F_y}–α characteristic (Edwards & Hogg 1968), and it has occurred with suspension bridge decks, including the Deer Isle Bridge in the United States which galloped in 1942 with a 3.8 m (12.5 ft) amplitude (Vincent 1965). It will occur for structural members (Slater 1969), and its potentially dangerous occurrence has occasionally been avoided by wind-tunnel tests on models in the design stage (McKillop 1968).

(*b*) *Effects of body and incident wind parameters*

The phenomena of figure 7 indicate that reattachment of the separated flow to the afterbody surface is an important characteristic of the galloping cycle, so the shape and streamwise length of the section afterbody are important parameters. The data, presented in figure 6, of Brooks (1960) and Smith (1962), obtained in galloping tests on cylinders of rectangular section with different b/h ratios, demonstrate this importance. For very small b/h, no transverse force develops at small angles of attack, and the section is stable at rest, although the sections will behave as hard oscillators and gallop to stable amplitudes if given a sufficient initial transverse velocity $\mathrm{d}y/\mathrm{d}t$ to make the short afterbody interact with the separated shear layers. For intermediate values of b/h the sections, including the square, gallop from rest, but with amplitudes at a given wind speed decreasing with increasing b/h. This behaviour results from the lower value of α for reattachment on the windward side in the galloping cycle as b/h is increased, until at about $b/h = 3.5$ reattachment occurs at $\alpha = 0$, and the section will not gallop.

Since any cross-section but the circle will display some variation of C_{F_y} with α, it follows that any such section will have a range or ranges of α for which $A = \mathrm{d}C_{F_y}/\mathrm{d}\alpha$ is positive. That more sections do not in fact gallop is explained by the low values of A usually found. The relation of A to structural parameters will be discussed in § 3*c*.

Effects of Reynolds number on galloping have not been investigated seriously. Many sections which gallop vigorously have fixed separation points, like the square, so separation for them is independent of *Re*. However, reattachment would still be *Re*-dependent, so the galloping characteristics should experience some effect.

Effects of mean velocity profile and turbulence in the wind on galloping have been investigated recently, and Novak (1968) has tested a model tower of square section in the presence of winds of 4.7 and 8.6 % turbulence intensity, and with mean velocity profiles typical of natural winds in open country and urban areas, respectively, to model scale. He found vigorous transverse galloping behaviour qualitatively similar to that observed for the same model in smooth flow, but quantitatively of decreasing amplitude with increasing turbulence. His galloping amplitude levels in turbulence, converted approximately to the different model test conditions of figure 9, are indicated there by dashed lines. The results suggest that a sufficient intensity of turbulence will suppress galloping. A probable explanation of the reduced galloping amplitudes with increasing turbulence is that the turbulence causes reattachment to the afterbody surface at lower angles of attack, so that increased turbulence behaves like increased b/h for the rectangular sections. Vickery (1965) has suggested that results of wind tunnel tests he carried out on a stationary square-section cylinder in a wind of uniform mean profile and 10 % turbulence intensity imply flow reattachment to the afterbody surfaces at $\alpha = 0$.

(*c*) *Methods of analysis and suppression*

For the analysis of transverse galloping, as for vortex-induced oscillations, the structural system can usually be considered linear, at least for low amplitudes, and, with the quasi-steady approximation to the aerodynamic excitation, the necessary empiricism is introduced as the static variation of C_{F_y} with α. Since $\tan\alpha = (1/V)\,(\mathrm{d}y/\mathrm{d}t)$, C_{F_y} is an empirical function of $\mathrm{d}y/\mathrm{d}t$, which can be approximated by a polynomial (Parkinson & Smith 1964), as shown for the square section in figure 8. This polynomial function for the excitation gives a weakly nonlinear differential equation of motion for the system, which can be solved by standard methods (Minorsky 1962), leading to the theoretical predictions of amplitude against wind speed and amplitude against time illustrated in figures 9 and 10. It can be seen that the theory gives good predictions of galloping characteristics. Essentially the same theory was developed independently some years previously for application to the stall flutter of airfoils (Sisto 1953), and Scruton (1960) has determined galloping amplitudes from empirical C_{F_y} data by a graphical method.

Means of suppressing or preventing transverse galloping are suggested by equation (6). If V_0 can be made higher than any wind speed expected for the structure, it will not gallop. Accordingly, for a given size of cross-section h, the shape can be modified to reduce A, the structure can be made stiffer to increase f_n, or the structural damping β can be increased and/or the density ratio n reduced to increase Δ. Which combination of these methods of preventing galloping is used depends of course on the compatibility of the changes with other features of the structure.

PHILOSOPHICAL TRANSACTIONS OF THE ROYAL SOCIETY A MATHEMATICAL, PHYSICAL & ENGINEERING SCIENCES

4. Future requirements and prospects

It is clear from the nature of modern structural design of long, slender structures, in which materials and construction methods combine to produce low natural frequencies and low structural damping, that the danger of undesirable vortex-induced oscillations or possibly catastrophic galloping will continue to be present, and will have to be countered by suitable criteria in the design stage. Bridge designers have been aware of the need to analyse for wind-induced instabilities since the Tacoma Narrows disaster, and most designers and architects for very tall buildings and other such slender structures now seem to realize the analogous need in connexion with their designs. Perhaps it will not be necessary for a skyscraper to gallop to drive the point home.

Of course being aware of the problem is only the first step. Designers need accurate information to permit them to establish quantitative criteria against wind-induced oscillations. On the structural side the greatest need is an improved ability to predict structural damping, for, of the controlling parameters discussed in §§ 2 and 3, the damping parameter is the one most likely to be at the disposal of the designer, and, if it could be predicted accurately, it would be extremely helpful.

Wind tunnel tests will continue as the main source of aerodynamic information. There is a clear need for more testing at higher Reynolds numbers, and, since there is evidence of the persistence of coherent vortex and galloping excitations in winds of mean profile and turbulence intensity simulating natural winds near the ground, there is a need for more testing for vortex-induced and galloping oscillations in such winds. Studies of this kind have been started in the author's laboratory, and elsewhere.

Since a good theory greatly reduces the amount of experimental work required, there is an obvious need for adequate theories for the organized (as opposed to the random) characteristics of separated flows, with and without motions of the generating bluff bodies. Progress is being made. For the vortex excitation problem, Abernathy & Kronauer (1961), Sarpkaya (1968), and others, have shown the usefulness of potential flow theory in modelling the near-wake vortex system and its excitation of the generating body. The work of Hartlen *et al.* (1968) referred to in § 2 suggests an analytical approach to the interplay between vortex excitation and structural response, and it is perhaps reasonable to hope for a theory, with a minimum of empiricism, marrying these two approaches.

For the galloping problem, if V_0 is appreciably greater than V^*, the quasi-steady approximation leads to good predictions of galloping behaviour, so that, for smooth flow at least, progress with the theory requires an analytical model for the stationary C_{F_y}–α behaviour. Since C_{F_y} depends on the time-average pressure distribution over the afterbody, perhaps the above potential flow vortex models will also prove useful here, by providing a basis for the calculation of time-average pressure distributions, again with a minimum of empiricism.

References (Parkinson)

Abernathy, F. H. & Kronauer, R. E. 1961 *J. Fluid Mech.* **13**, 1–20.
Bishop, R. E. D. & Hassan, A. Y. 1964 *Proc. Roy. Soc. Lond.* A **277**, 51–75.
Brooks, N. P. H. 1960 M.A.Sc. Thesis, University of British Columbia.
Davenport, A. G. 1961 Ph.D. Dissertation, Bristol.
Davis, D. A., Richards, D. J. W. & Scriven, R. A. 1963 *Proc. Inst. Elect. Engrs* **110**, 205.
Edwards, A. T. & Hogg, A. D. 1968 *Proc. Int. Res. Seminar. Wind Effects on Buildings and Structures, Ottawa* **1**, 231–244.

PHILOSOPHICAL TRANSACTIONS OF THE ROYAL SOCIETY A MATHEMATICAL, PHYSICAL & ENGINEERING SCIENCES

Farquharson, F. B., Smith, F. C. & Vincent, G. S. 1949–54 *Expl Station Bull.* **116**, parts I–V. University of Washington.
Feng, C. C. 1968 M.A.Sc. Thesis, University of British Columbia.
Ferguson, N. & Parkinson, G. V. 1967 *ASME Jl Engrg Industry* **89**, 831–838.
Fung, Y. C. 1955 *An introduction to the theory of aeroelasticity*. New York: Wiley.
Gerrard, J. H. 1966 *J. Fluid Mech.* **11**, 244–256.
Glauert, H. 1919 *British Government Aeronautical Research Council, R. & M.* 595.
Hartlen, R. T., Baines, W. D. & Currie, I. G. 1968 *Report UTME-TP* 6809. University of Toronto.
den Hartog, J. P. 1930 *Trans. A.I.E.E.* **49**, 444.
Holownia, B. P. 1968 *Proc. Symp. Wind Effects on Buildings and Structures, Loughborough University* **2**, Paper 35.
Johns, D. J. & Allwood, R. J. 1968 *Proc. Symp. Wind Effects on Buildings and Structures, Loughborough University* **2**, Paper 28.
Koopmann, G. H. 1967 *J. Fluid Mech.* **28**, 501–512.
McKillop, J. A. 1968 *Proc. Int. Res. Seminar. Wind Effects on Buildings and Structures, Ottawa* **1**, 371–398.
Nakagawa, K., Fujino, T., Arita, Y. & Shima, T. 1965 *Proc. Symp. Wind Effects on Buildings and Structures, N.P.L.* **2**, 774–795.
Novak, M. 1968 Report BLWT–7–68, University of Western Ontario.
Parkinson, G. V. & Smith, J. D. 1964 *Q. Jl. Mech. appl. Math.* **17**, 225–239.
Roshko, A. 1954 NACA TN 3169.
Roshko, A. 1961 *J. Fluid Mech.* **10**, 345–356.
Santosham, T. V. 1966 M.A.Sc. Thesis, University of British Columbia.
Sarpkaya, T. 1968 *Proc. Symp. Unsteady Flow*. American Society of Mechanical Engineers.
Scruton, C. 1960 Agard report 309.
Scruton, C. 1965 *Proc. Symp. Wind Effects on Buildings and Structures, N.P.L.* **2**, 797.
Scruton, C. 1968 *Proc. Int. Res. Seminar. Wind Effects on Buildings and Structures, Ottawa* **1**, 115–162.
Scruton, C. & Walshe, D. E. J. 1957 N.P.L. Aero Report 335.
Simpson, A. & Lawson, T. V. 1968 *Proc. Symp. Wind Effects on Buildings and Structures, Loughborough University* **2**, Paper 25.
Sisto, F. 1953 *J. Aero. Sci.* **20**, 598–604.
Slater, J. E. 1969 Ph.D. Thesis, University of British Columbia.
Smith, J. D. 1962 M.A.Sc. Thesis, University of British Columbia.
Toebes, G. H. 1969 *ASME Jl Basic Engrg* **91**, 493–502.
Vickery, B. J. 1965 N.P.L. Aero Report 1146.
Vincent, G. S. 1965 *Proc. Symp. Wind Effects on Buildings and Structures, N.P.L.* **2**, 512–515.
Walshe, D. E. 1965 N.P.L. Aero Report 1107.
Wootton, L. R. 1968 N.P.L. Aero Report 1267.

PHILOSOPHICAL TRANSACTIONS OF THE ROYAL SOCIETY A MATHEMATICAL, PHYSICAL & ENGINEERING SCIENCES

Discussion: critical wind speeds for suspension bridges

D. Dicker (*College of Engineering, State University of New York at Stony Brook, New York* 11790, *U.S.A. and Imperial College of Science and Technology, London*)

Over the past few years my work has dealt with the theory of aeroelastic stability of suspension bridges, and what I would like to very briefly outline this afternoon is a further development in my work, which extends somewhat material on the subject I presented to the American Society of Civil Engineers at the national meeting in April 1969 (Dicker 1969).

The point of departure of my work from most other work on the subject can be explained, I believe, most easily in terms of the function which is assumed to describe the motion of a suspension bridge deck

$$e^{(-p+i\omega)t},$$

which may represent a vertical, angular or even possibly a horizontal displacement of the deck. The implicit argument is that as long as $p > 0$ the above is a damped sine or cosine term, and hence the motion is stable. And, if p is negative then the converse is true, i.e. the motion is unstable.

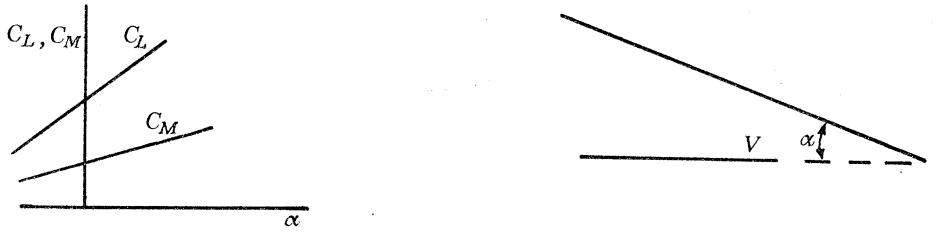

Figure 1

Based on this hypothesis, the critical point is then clearly $p = 0$, at which point the motion is purely oscillatory, and which represents the onset of instability. This is identical with the assumption in classical flutter theory that the basic driving mechanism is some sort of oscillation, but which for suspension bridges at least, has never really been justified.

In my work I allow for the possibility of non-oscillatory motion simply by not prejudging the form of solution. What is assumed, however, is that because the motions of the structure are comparatively slow, one may use a quasi-steady approach by taking for the aerodynamic coefficients, namely the lift and moment, the static values. The resulting theory is quasi-steady because the angle of attack, or inclination, and vertical displacement change with time, and therefore so do the coefficients.

From numerous static tests on unstiffened and truss-stiffened suspension bridge sections, it is well known that the coefficient of lift against inclination approximates to a straight line for some range of inclinations, ± 3 or $4°$ (see figure 1*a*, *b*), and the moment coefficient is a similar curve. Clearly then in this range we may write:

$$C_L = C_{L_0} + A\alpha,$$

$$C_M = C_{M_0} + B\alpha.$$

In my earlier paper (Dicker 1969), it was shown that the bridge cables behave as linear springs for small applied loads so that representing an unstiffened bridge section as shown in figure 2, we obtain the equations of motion of the deck

$$M\ddot{u} + ku = [C_{L_0} + A(\alpha - \dot{u}/V)]\,\tfrac{1}{2}\rho V^2 b, \tag{1}$$

$$I\ddot{\alpha} + \tfrac{1}{2}k\alpha = [C_{M_0} + B(\alpha - \dot{u}/V)]\,\tfrac{1}{2}\rho V^2 b^2, \tag{2}$$

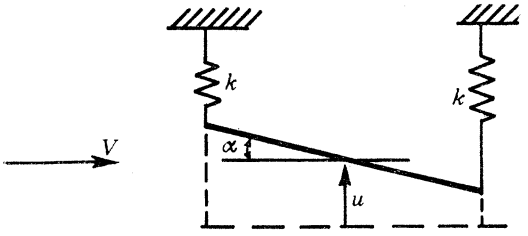

FIGURE 2

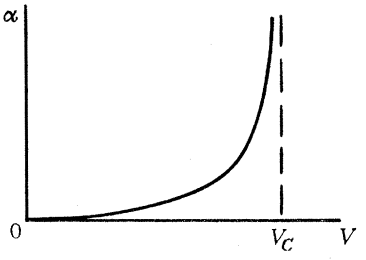

FIGURE 3

where M, I and k are the effective mass and polar moment of inertia of the deck and the spring constant of the cables respectively. The motion of the section relative to the airstream has been accounted for in these expressions.

From these equations there follow some rather interesting results and conclusions. Considering first pure torsional or angular motion, which is the mode associated with catastrophic instability, we note that for any wind speed there is a corresponding angular equilibrium configuration, which we get from the second equation by setting to zero all derivative terms, and which is

$$\alpha = \frac{C_{M_0}\rho V^2 b^2}{k - BPV^2 b^2}.$$

Clearly for some particular value of wind speed the denominator vanishes indicating an instability of the divergence type. The curve of inclination against wind speed is sketched in figure 3 where the critical wind speed, V_c, appears as an asymptote. Further, it may easily be shown that large amplitude oscillations should be anticipated even for this mode of failure. In this analysis it was assumed that the wind was steady, which is, of course, never the case. Consider the effect of a small disturbance to a steady wind, a spike or delta function of magnitude C, at $t = t_0$ (figure 4). Rewriting the differential equation for torsional motion alone about the equilibrium configuration just before the disturbance we have

$$I\ddot{\alpha} + [\tfrac{1}{2}k - B\tfrac{1}{2}\rho v^2 b^2]\,\alpha = 0,$$

$$\alpha(t_0^-) = \alpha_0,$$

$$\dot{\alpha}(t_0) = 0,$$

and substituting $V_0^2 + C\delta(t-t_0)$ for V^2 in the differential equation results in a solution which includes a term

$$(C/W_f)\sin W_f t,$$

where W_f is the bracketed term in the differential equation divided by I and which decreases with increasing V. Clearly, for a disturbance of the same magnitude, the amplitude of motion becomes much larger as the wind speed approaches the critical value. Hence, what the observer sees is not simply a deck rolling over as the critical wind speed is approached, but a series of oscillations of increasing amplitude. But the mechanism is, nevertheless, a divergence. Moreover, it should be noted that there is no possibility of aerodynamic damping with this type of motion.

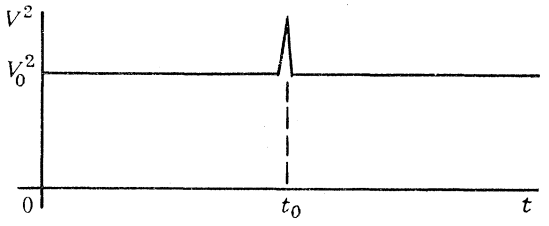

FIGURE 4

Critical wind speeds have been computed by Dicker (1969) for two actual suspension bridges of the unstiffened type: the Wheeling Bridge in West Virginia, and the George Washington Bridge before the addition of the second deck. These turn out to be 15 m s^{-1} (34 mi/h) for the Wheeling Bridge and 37 m s^{-1} (82 mi/h) for the George Washington Bridge. A significant point is that, a few years after its completion, the Wheeling did, in fact, blow down.

While I am quite sure that the divergent mode just described is the most critical in suspension bridge design, one should take account of the non-catastrophic bridge motion which occurs in a narrow range of rather low wind speeds and reported by several people and noted a few years ago on the model tests of the Severn Bridge.

This phenomenon too may be explained in terms of the differential equations (1) and (2). Rewriting these in terms of motions about the equilibrium configurations associated with a particular wind speed, and assuming for the moment that we may neglect the term $\dot{u}/V$ as compared with α on the right-hand side gives

$$M\ddot{u} + ku = [A\tfrac{1}{2}\rho v^2 b]\,\alpha, \tag{3}$$

$$I\ddot{\alpha} + [\tfrac{1}{2}k - B\tfrac{1}{2}\rho V^2 b^2]\,\alpha = 0. \tag{4}$$

These are uncoupled in that (4) may be solved to give

$$\alpha = D\sin W_f t, \quad D = \text{const},$$

which may then be used to solve for u from (3). The important term in the solution is

$$u = \frac{(A\rho V^2 bD)/2M}{(k/M) - W_f^2}\sin W_f t.$$

Hence we see that there exists a true flutter mode where the torsional motion contributes to the instability of the vertical motion. It may be shown without too much difficulty that this critical speed is always lower than the critical speed at divergence. However, from (1) we see that by not discarding the term $\dot{u}/V$, which is, in fact, on the same order of magnitude as α, equation (1)

includes a damping term whose coefficient actually increases—causing stronger damping—as the wind speed increases.

The resultant curves of amplitude against wind speed for an unstiffened suspension bridge are thus of the form.

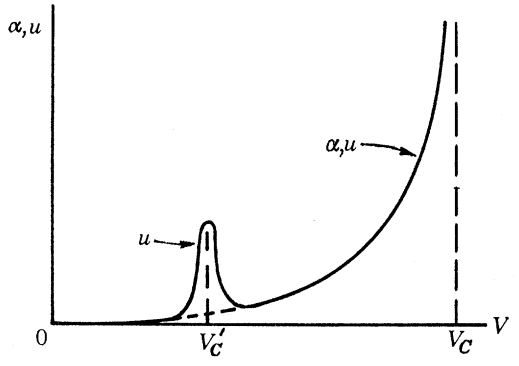

FIGURE 5

Hence, the linear analysis appears to be sufficient not only for the quantitative prediction for design purposes of catastrophic (divergent) suspension bridge motion, but non-catastrophic (flutter) motion as well.

REFERENCE (Dicker)

Dicker, D. 1969 Aerodynamic stability of unstiffened suspension bridges, Preprint 851, A.S.C.E. Annual Meeting and National Meeting in Structural Engineering, Louisville, Kentucky, April 1969.

PHILOSOPHICAL TRANSACTIONS OF THE ROYAL SOCIETY A MATHEMATICAL, PHYSICAL & ENGINEERING SCIENCES

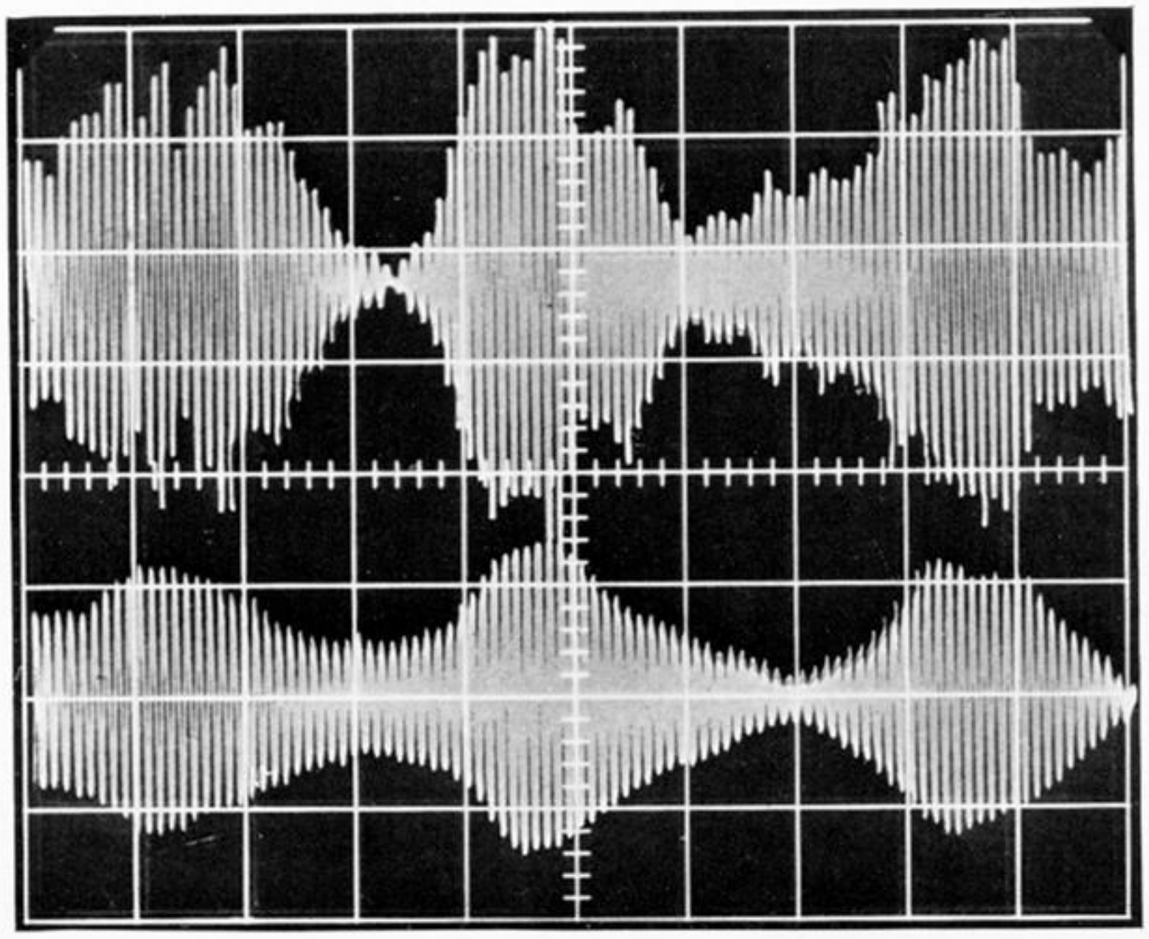

2

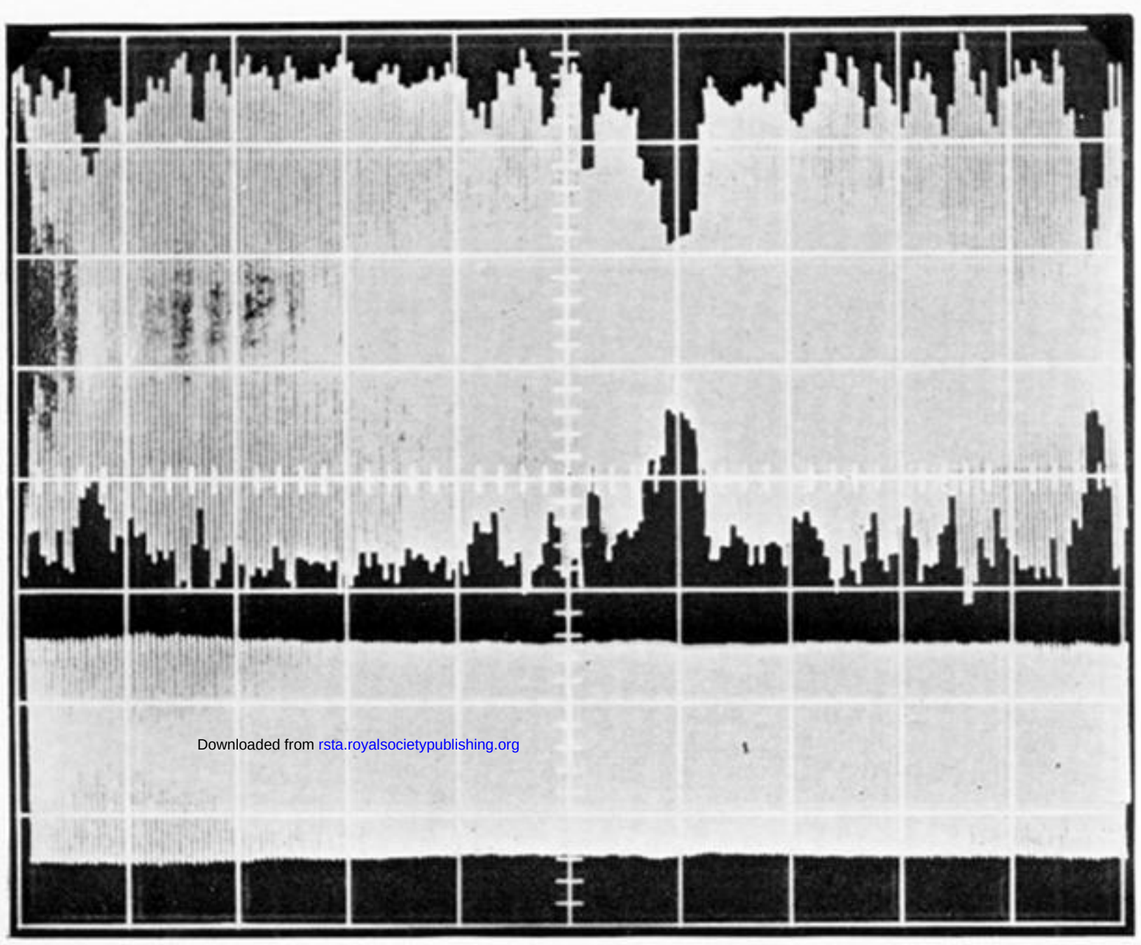

3*a*

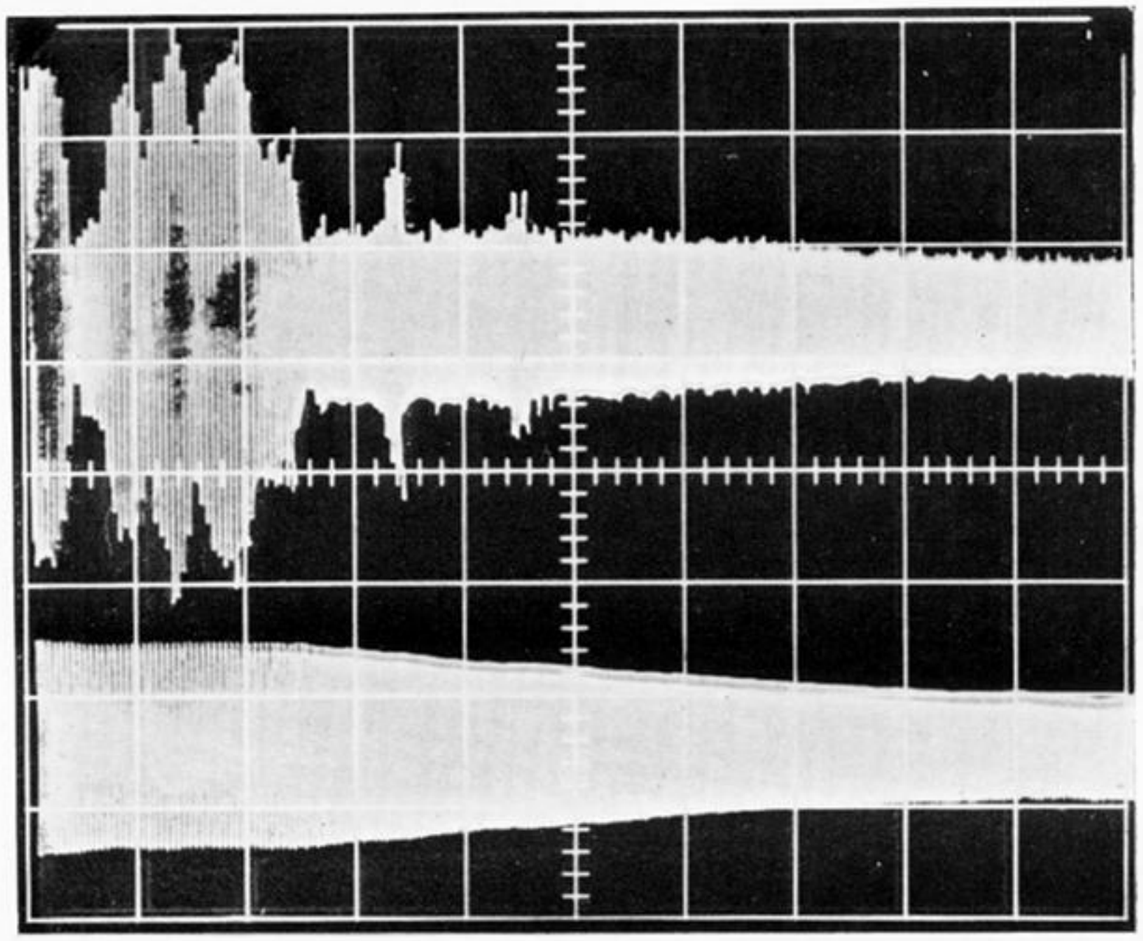

3*b*

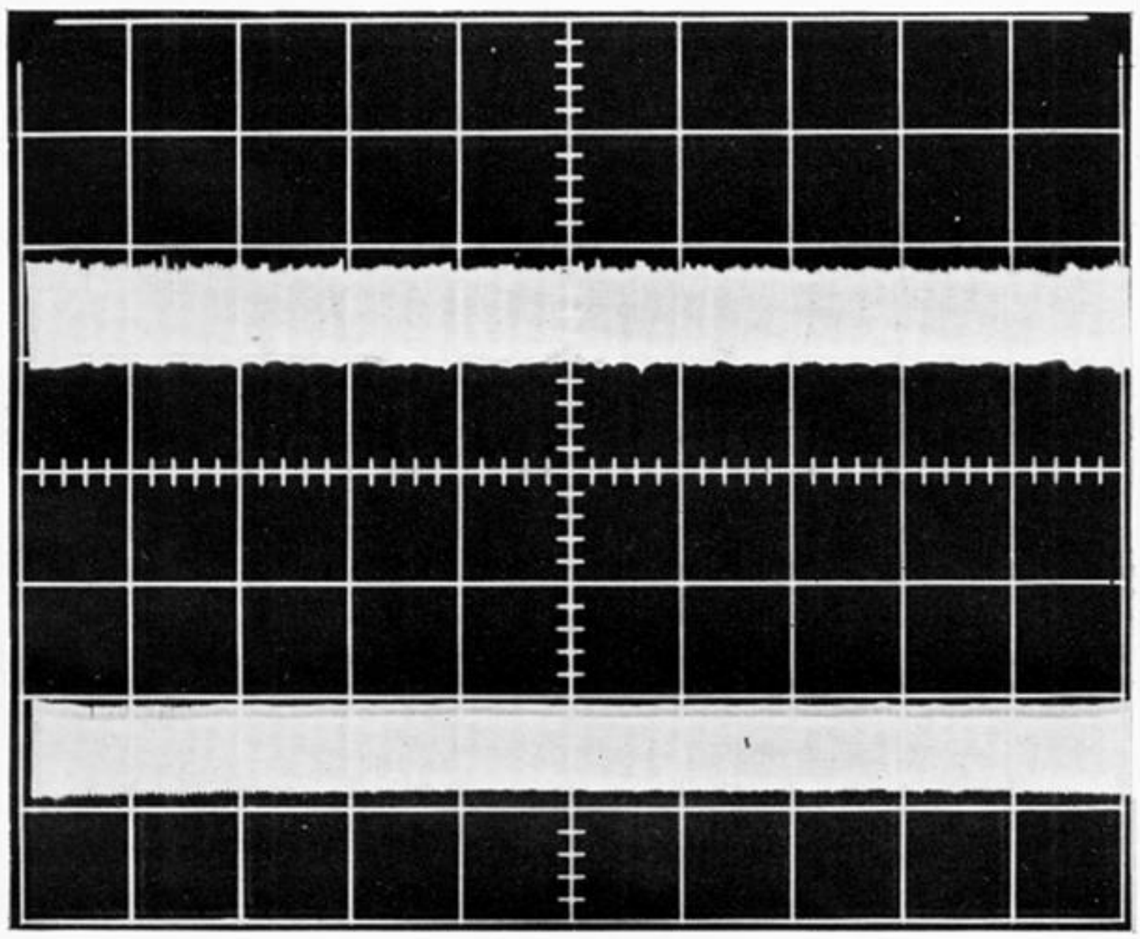

c

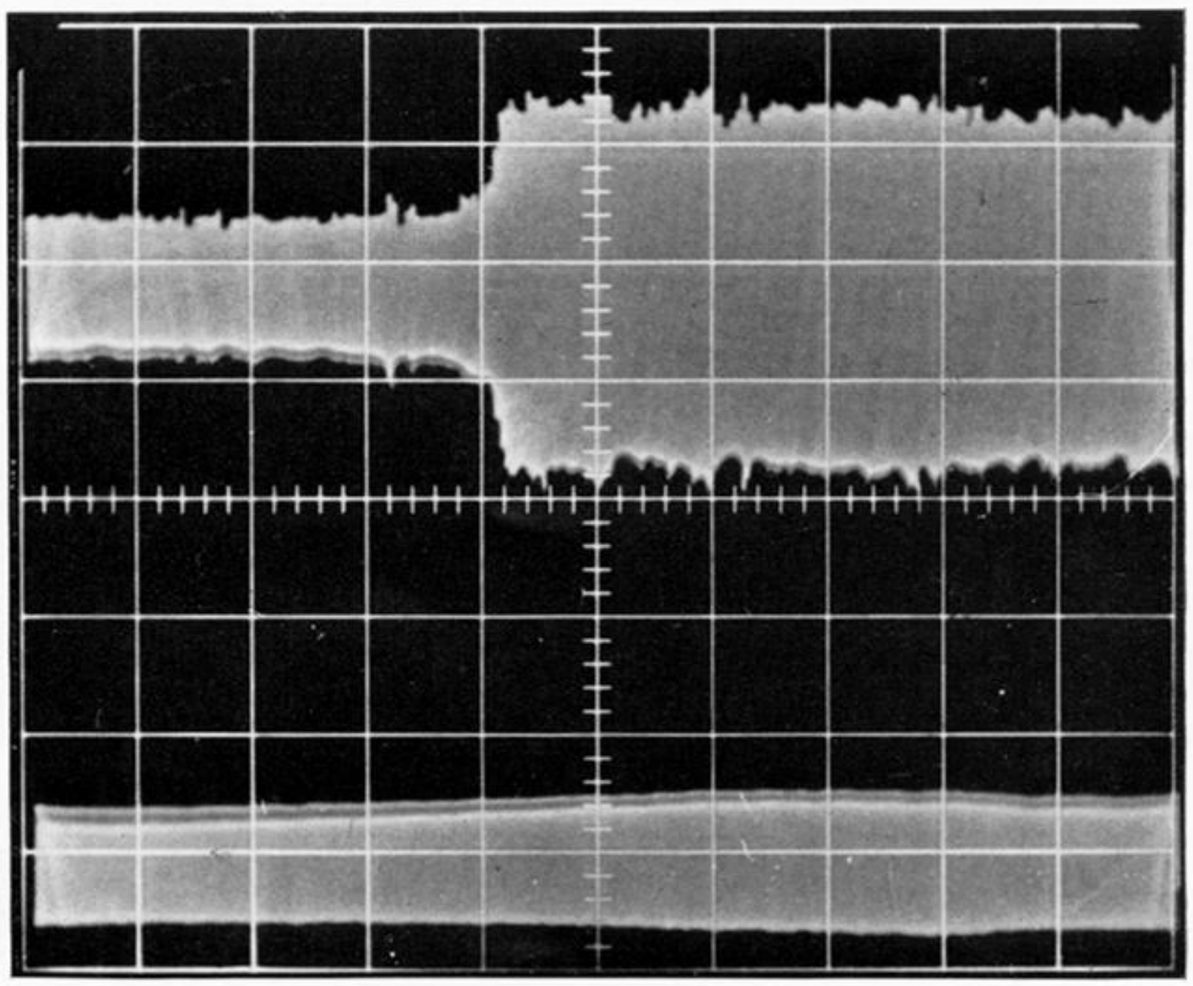

3*d*

FIGURE 2. Beat phenomenon. $V/f_n h = 4.97$. Upper trace: surface pressure at transverse tap, $f_{v_0} = 8.73$ Hz. Lower trace: cylinder displacement, $f_c = 9.04$ Hz. Time base: 1 s/division.

FIGURE 3. Transient effects on cylinder and surface pressure amplitudes during capture. Upper traces: surface pressure at transverse tap, $f_{v_0} = 9.04$ Hz. Lower traces: cylinder displacement, $f_c = 9.04$ Hz. Time base: 2 s/division. (*a*) $V/f_n h = 6.33$; (*b*) $6.33 < V/f_n h < 6.68$. (*c*) $V/f_n h = 6.68$. (*d*) $6.11 > V/f_n h > 5.89$.